

## Analysis of potential landslide processes in the Passo della Morte (Carnian Alps, Italy)

Lesław ZABUSKI<sup>1,\*</sup> and Gianluca MARCATO<sup>2</sup>

<sup>1</sup> Polish Academy of Sciences, Institute of Hydro-Engineering, Kościarska 7, 80-328 Gdańsk, Poland

<sup>2</sup> National Research Council, Research Institute for Geo-Hydrological Protection, Corso Stati Uniti 4, 35127 Padova, Italy



Zabuski, L., Marcato, G., 2020. Analysis of potential landslide processes in the Passo della Morte (Carnian Alps, Italy). *Geological Quarterly*, **64** (3): 681–691, doi: 10.7306/gq.1552

Numerical simulations are provided of a potential landslide on a slope in the Passo della Morte (Carnian Alps, northeastern Italy). The slope is situated on the flank of a valley of the Tagliamento River. The danger arising from the potential landslide is associated with sliding rock damming the valley and a sudden discharge of water accumulated at the back of the dam in the case of its uncontrolled outburst. A description of the geology and geomechanical properties of the rock mass provides context for analysis of four models differing in terms of the shapes and dimensions of the solid rock blocks. The Universal Distinct Element Code (UDEC) is used to simulate the landslide of the rock mass modelled as a set of blocks interacting along discontinuities. Deformation scenarios obtained in the simulations vary depending on the model. Different, both continuous and discontinuous, deformation and failure mechanisms such as buckling, rockfall, rotation of the individual blocks and their packets, and folding, take place in each of the models analysed. Nevertheless, slip movement occurs in all four models. In addition, the simulations show that the rock mass in the deformed zones undergoes strong loosening.

Key words: Passo della Morte landslide, discontinuous rock mass, distinct element method.

### INTRODUCTION

We describe the numerical modelling and simulation of a potential landslide process at the Passo della Morte (Carnian Alps, northeastern Italy; Fig. 1). The numerical code UDEC (Universal Distinct Element Code: Itasca C.G., 2004) was used, which enables performance of such simulation for discontinuous media, based on the distinct element method (Starfield and Cundall, 1988; Giani, 1992; Marcato et al., 2005, 2007; Zabuski and Marcato, 2014; Cundall and Hart, 2014; Bossi et al., 2016). The rock mass is modelled as a set of solid rock blocks, interacting along discontinuities. Discontinuities, as “a weakest link of the chain” play a fundamental role in the development of the deformation processes of the rock masses (Hoek and Bray, 1981).

The objectives of the analysis were to investigate:

- the potential landslide process, from initiation to the advanced stages of displacement,
- the possible (virtual) deformation mechanisms,
- the influence of the assumed shape and dimensions of the intact rock blocks on the deformation process,
- the influence of the geomechanical parameters of discontinuities on the landslide process.

It should be pointed out that the landslide processes analysed in the paper have not still taken place in reality and are only potential.

### SLOPE MODELS

#### GENERAL DESCRIPTION AND STRUCTURAL MODELS OF THE SLOPE

The Passo della Morte (PdM) site is situated on the left flank of a narrow Alpine valley in northeastern Italy, ~3 km to the east of the village of Forni di Sotto (Lon. 12.7026, Lat. 46.3978; Fig. 1). The Tagliamento River flows eastwards at the bottom of the valley. The site consists of an unstable rock mass, as indicated by its history of failures, that occupies elevations between 900 m above sea level (a.s.l.) and the toe of the slope at 620 m a.s.l. Between the elevation of 650 m and the toe of the slope the rock is hidden by coarse loose deposits accumulated by small-scale rock falls. The rock spur is ~130 m wide. A road tunnel crosses the unstable rock mass for its entire width at a constant elevation of 720 m a.s.l. with shallow cover (0–15 m) on the side towards the slope. As can be observed on the geological map of the area in Figure 2 and in the cross-section in Figure 3, the outcropping units at the Passo della Morte are a thick-bedded dolomite (Dolomia dello Schlern – Ladinian), which constitutes the bedrock, and a thinly stratified limestone (Calcari scuri stratificati – Carnian) which overlies the dolomite with a steep contact. The dolomite and limestone rest on silty clays (Argille siltose varicolori – Middle Carnian) which are present at the base of the slope and are covered by loose debris detached from the upper slopes (Fig. 4).

\* Corresponding author, e-mail: [lzabuski@wp.pl](mailto:lzabuski@wp.pl)

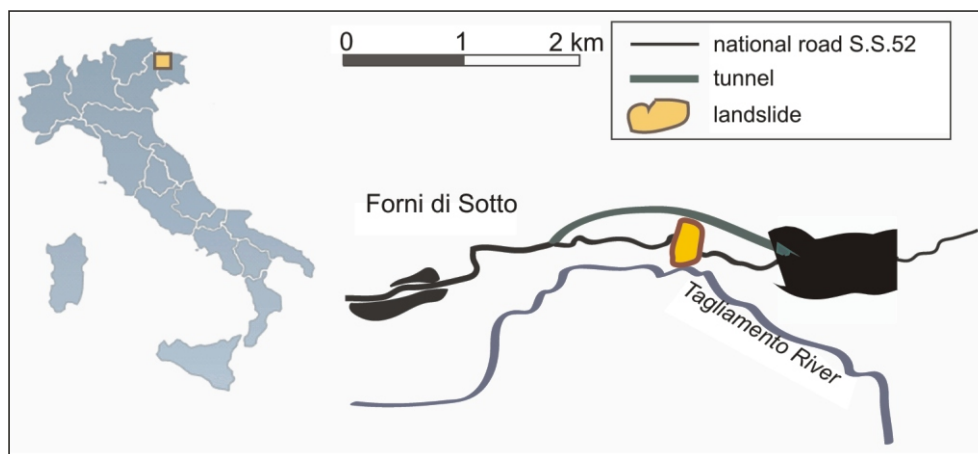


Fig.1. Site location in the Carnian Alps (NE Italy)

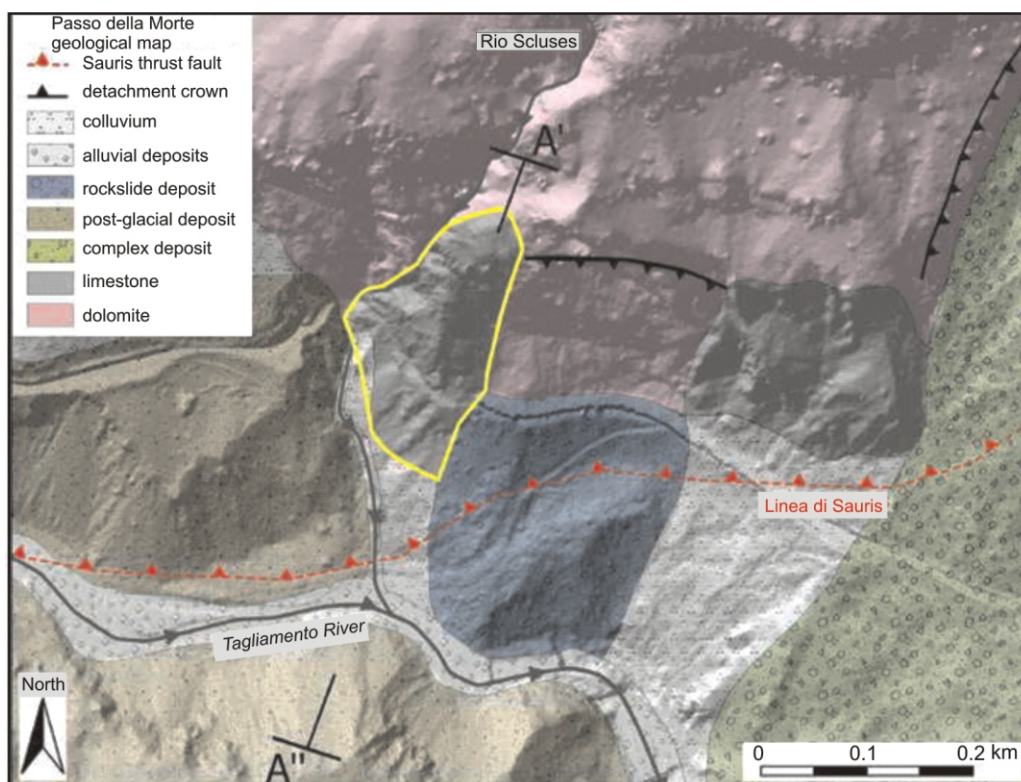


Fig. 2. Bedrock geology and superficial deposits map of the Passo della Morte site

The unstable limestone outcrop (landslide) is highlighted in yellow; A'-A'' indicates the approximate location of the cross-section in Figure 3 (after Codeglia, 2017)

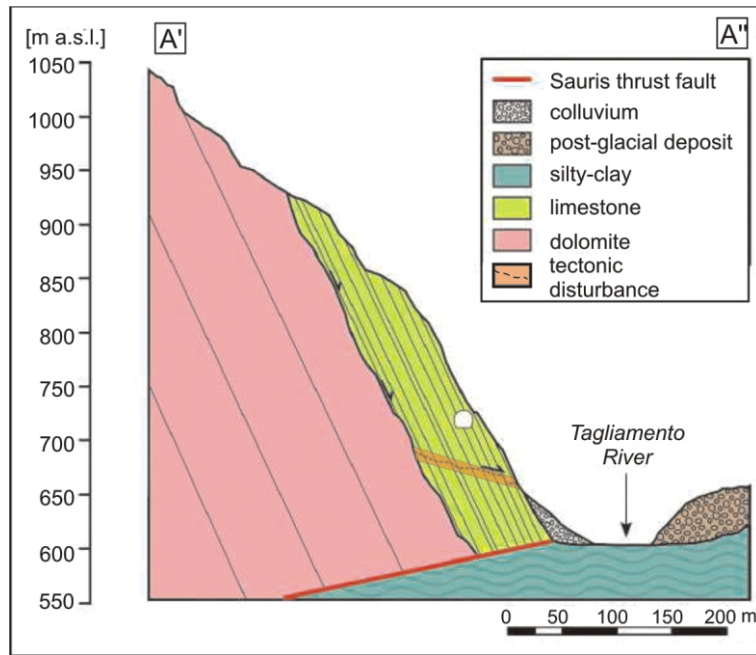


Fig. 3. Indicative cross-section of the Passo della Morte (Codeglia, 2017)

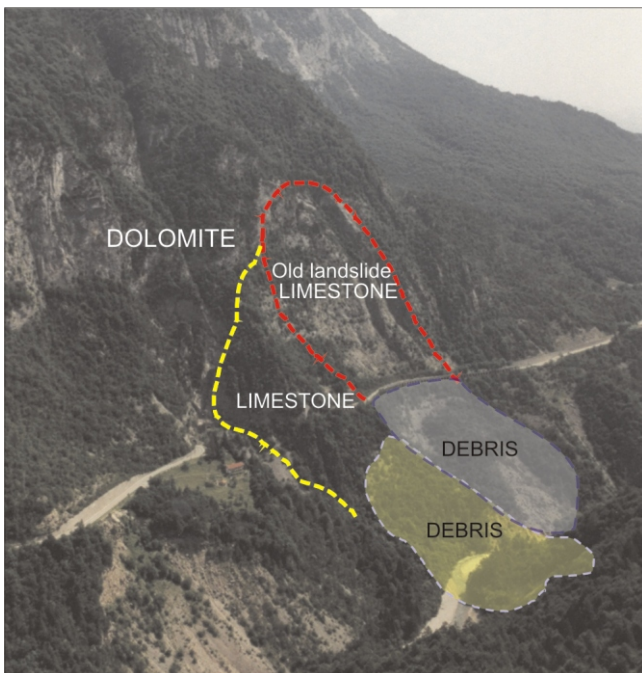


Fig. 4. View of the slope towards the NE with the region of the potential landslide (yellow line)

The rock mass has the potential to mobilise  $\sim 650,000 \text{ m}^3$  of material in the case of collapse of the whole unit (Codeglia, 2013; Codeglia et al., 2017). The site threatens the downstream villages through the potential for valley damming and consequent sudden discharge of the water accumulated at its back by the river, if dam outburst would occur (Codeglia, 2013).

The construction of the geomechanical model used for the numerical analysis was based on observations and measurements made on the southwestern rock mass face (Fig. 5). This

face approximately coincides with the cross-section analysed. The limestone strata, and the joints associated with the stratification, dip at  $73^\circ$  to the south-east, in the direction of the river valley. Joints are undulated and filled with weathered marlstone, from few millimetres to a maximum 25 cm in thickness.

Additional information concerning the rock mass structure and possible failure was obtained on the basis of the data collected by extensometers and inclinometers. The rock mass quality was described using the Rock Quality Designation (RQD) index (Bieniawski, 1984) determined on the basis of the rock core inspection from borehole S2 which is located within the tunnel at 720 m a.s.l. Results of extensometer measurements lead to the conclusion that changes in the discontinuity apertures have a local character and only extensometer no.4 showed displacements (Fig. 6).

Information concerning deformation structures within the rock mass was obtained from the results of inclinometer I22 (Fig. 7). The cumulative measured displacement was approximately 35 mm/6 months, beginning from 40-50 m below the tunnel level. It corresponds with low RQD values at depths between 47 and 50 m below the level of the tunnel (see Fig. 7). The shape of the inclinometer curve shows that a single distinct sliding surface does not exist and slides occur between multiple limestone layers.

#### GEOMECHANICAL AND NUMERICAL MODELS OF THE SLOPE

Four models of the rock mass were analysed, which differ in the shape and dimensions of the “elementary” rock blocks in the limestone bedrock (modeled blocks in the dolomite are much larger as this part of the slope does not take part in the landslide process and can be disregarded). An elementary block is created by two sets of discontinuities namely: bedding and joint set I, perpendicular to each other (Table 1). In model I square blocks of 3 × 3 m dimension were assumed. The elementary block in model II is rectangular in shape with dimensions of 1.75 × 6.8 m (Fig. 8). Dimensions of the blocks in model III are 1.75 × 6.8 m (the same as in model II), but the density of

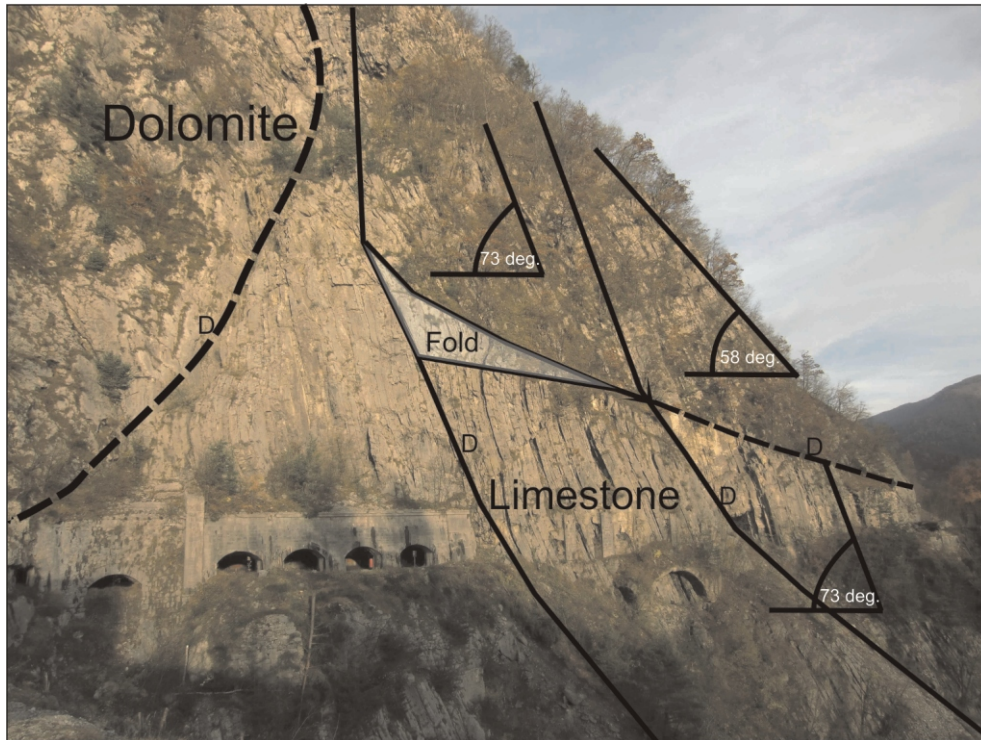


Fig. 5. Southwestern rock mass face with structures included into geomechanical models

D – discontinuity

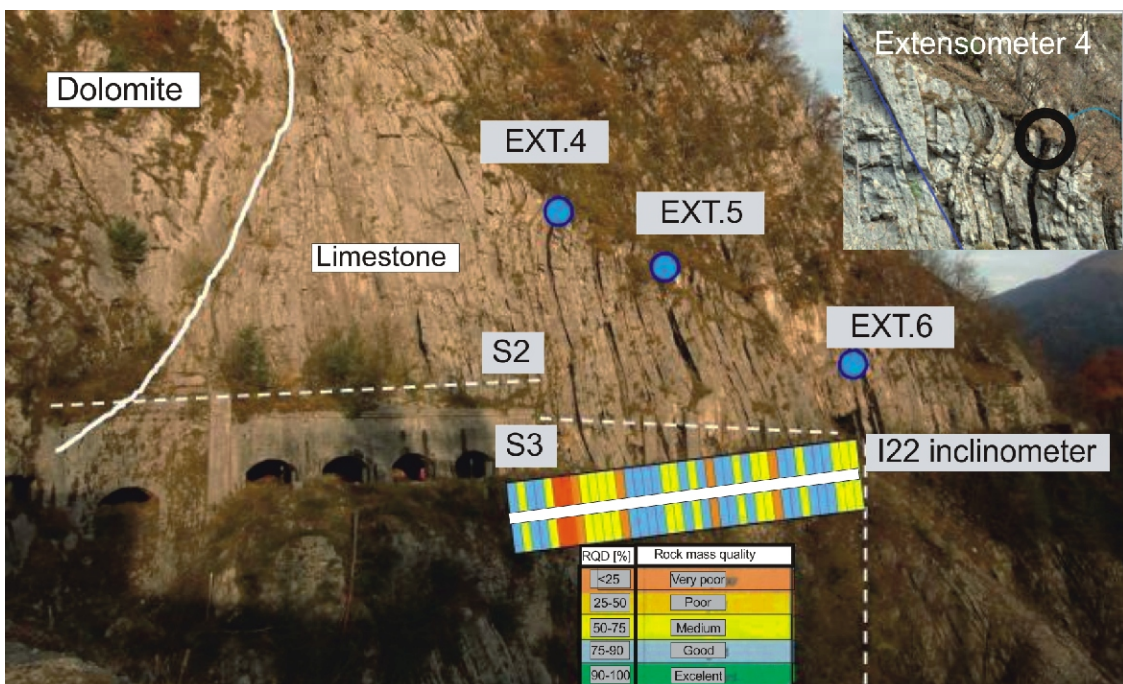


Fig. 6. Outcrop with the measuring devices and diagram showing the RQD index determined in Borehole S2 located within the tunnel

EXT.4, 5, 6 – extensometers; S2,S3 – boreholes

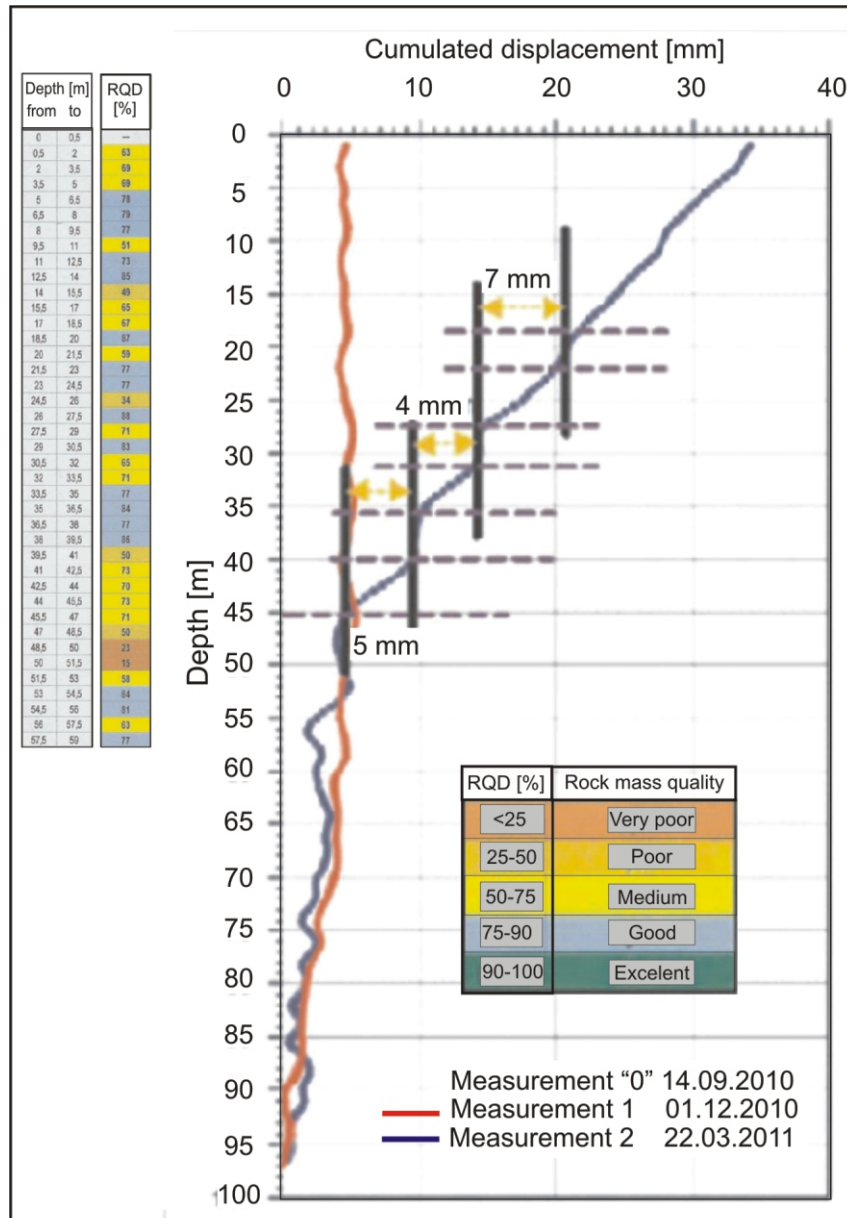


Fig. 7. RQD index distribution and displacement measured within inclinometer I22

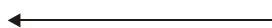


Fig. 8. Rectangular elementary block of intact rock in the limestone zone

Table 1

Joint set orientations and elementary block dimensions

	Model I	Model II	Model III	Model IV
Bedding, dip/dip direction (°) (spacing [m])	90/73 [3]	90/73 [1.75]	90/73 [1.75]	90/73 [1.75]
Joint set 1, dip / dip direction (°) (spacing [m])	0/17 [3]	0/17 [6.8]	0/17 [6.8]	0/17 [6.8]
Joint sets in tectonic and debris zones dip /dip direction (spacing [m])	None	None	65 25 [3]	73 17 [3]
Resulting elementary block – imestone and dolomite [m]	3 3	1.75 6.8	1.75 6.8	1.75 6.8
Resulting elementary block – tectonic and debris zones [m]	3 3	1.75 6.8	1.75 6.8	3.4 1.75

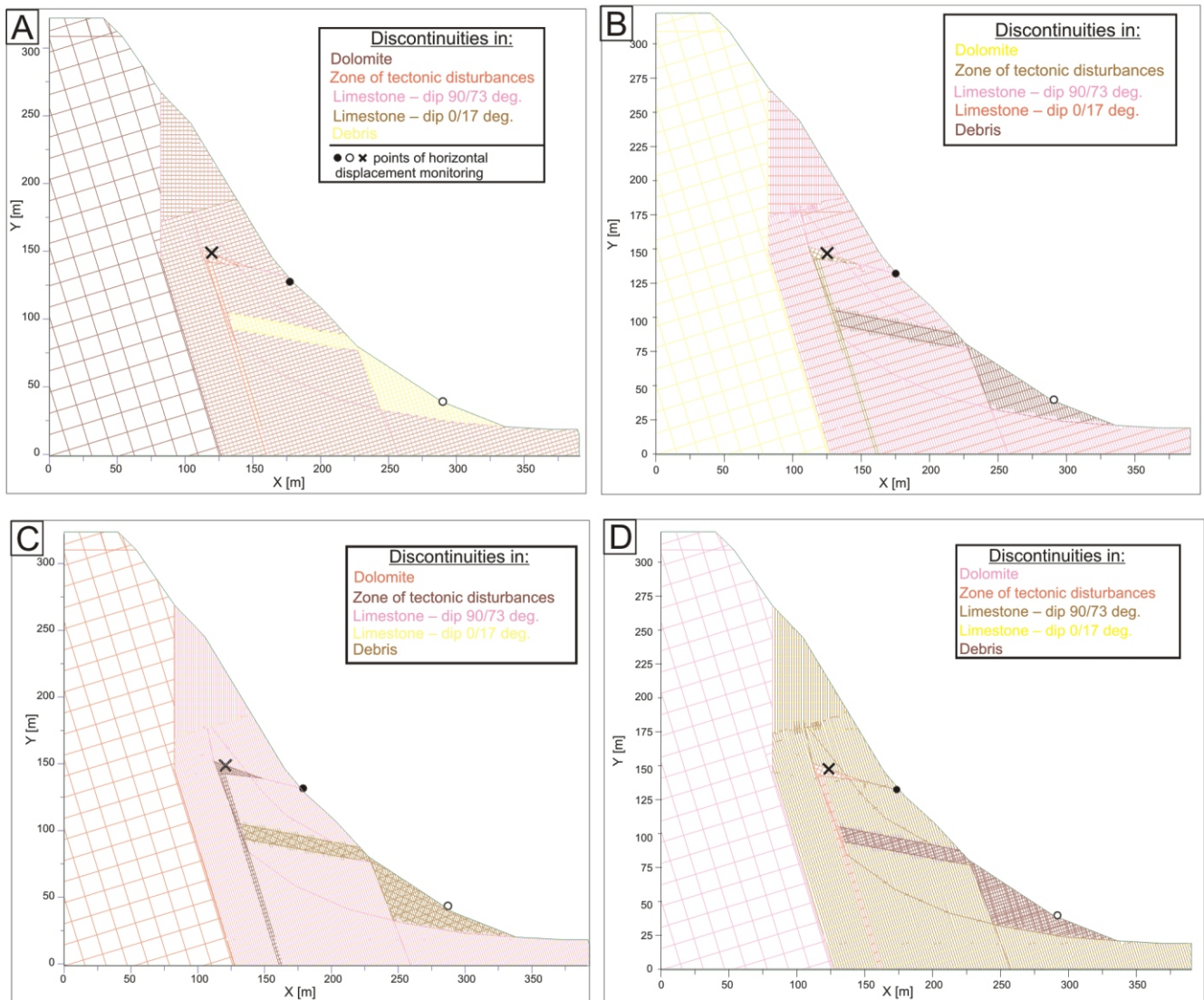


Fig. 9. Analysed models of the slope: A – model I, B – model II, C – model III, D – model IV

Different colours of the same layers in figures result from their automatic generation by the computer program; change of colour “by hand” is impossible

Table 2

**Geomechanical parameters of the rock (elastic model)**

Rock	Density [t/m <sup>3</sup> ]	Bulk modulus [GPa]	Shear modulus [GPa]
Limestone	2.3	1000	200
Dolomite	2.6	2000	500
Debris	2.3	200	50
Tectonic zone	2.2	10	5

Table 3

**Geomechanical parameters of discontinuities – model I and III**

Layer	Normal stiffness [GPa/m]	Shear stiffness [GPa/m]	Friction angle [°]	Cohesion [kPa]	Uniaxial tension strength [kPa]	Dilatation angle [°]
Limestone. Dip of discontinuities joint set 1 – 0/17° *	500	20	15.0	30	5	4
Limestone. Dip of bedding 90/73°	50	2	10.0	15	0	0
Dolomite	5000	2000	55	10000	100	0
Debris	10	5	35	0	0	8
Tectonic zone	20	10	8	5	0	0

\* – first number is dip angle of discontinuities in the upper part of the slope and the second number designates the dip angle in the lower part

Table 4

**Geomechanical parameters of discontinuities – model II and IV**

Layer	Normal stiffness [GPa/m]	Shear stiffness [GPa/m]	Friction angle [°]	Cohesion [kPa]	Uniaxial tension strength [kPa]	Dilatation angle [°]
Limestone. Dip of discontinuities joint set 1 – 0/17°	500	20	15.0	30	5	4
Limestone. Dip of interbedding discontinuities 90/73°	10*	1	10.0	5	0	0
Dolomite	5000	2000	55	10000	100	0
Debris	5	1	28	0	0	8
Tectonic zone	20	10	8	5	0	0

\* – parameters changed

discontinuities in the zone of tectonic disturbance and in the debris zone – shown in Figure 9 – is significantly larger. These zones are characterized by increased fragmentation and smaller dimensions of the blocks and thus additional joints are introduced, creating such fragmentation. The dimensions of a block in the fourth (IV) model in the limestone zone is the same as in the second one, but these dimensions in the zone of tectonic disturbances and debris are 3.4 – 1.75 m. Despite this regular division of the rock mass into elementary blocks, a few discontinuities (visible in Fig. 5 and marked by the letter “D”) were introduced in the model. They express the splitting of the slope into zones with different kinds of rocks and densities of discontinuities. All four models generated by the UDEC are shown in Figure 9. Geomechanical parameters of the intact rock, identical in all models, are set out in Table 2 while the parameters of discontinuities differ among the models and are reported in Ta-

bles 3 and 4. These parameters were assumed based on expert knowledge and on the literature (e.g., Hoek and Bray, 1981; Giani, 1992), as laboratory tests of specimens of undisturbed discontinuities were impossible since sample extraction from the rock mass was extremely difficult and even dangerous.

Moreover, the aim of the analysis was to describe possible mechanisms of slope failure and not to assess slope stability.

## RESULTS OF THE ANALYSIS

In the numerical analysis of the four models introduced above, the numerical simulations were stopped after an arbitrary amount of time steps had passed, and prior to convergence of the iteration process. This means that the simulated landslide process had not yet reached equilibrium when the

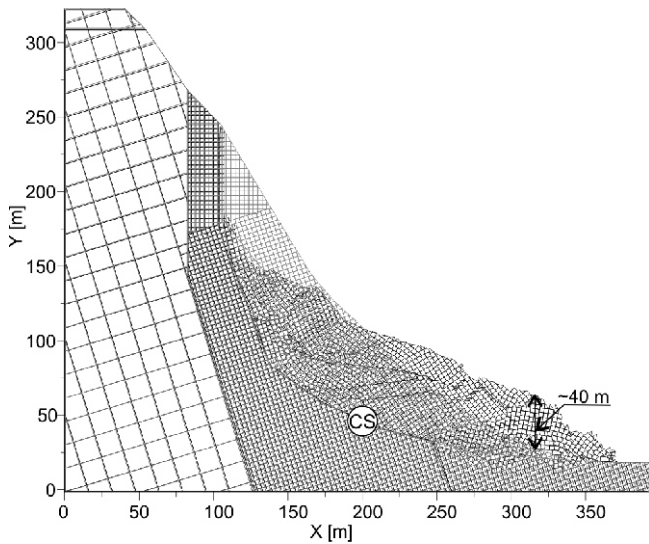


Fig. 10. Model I

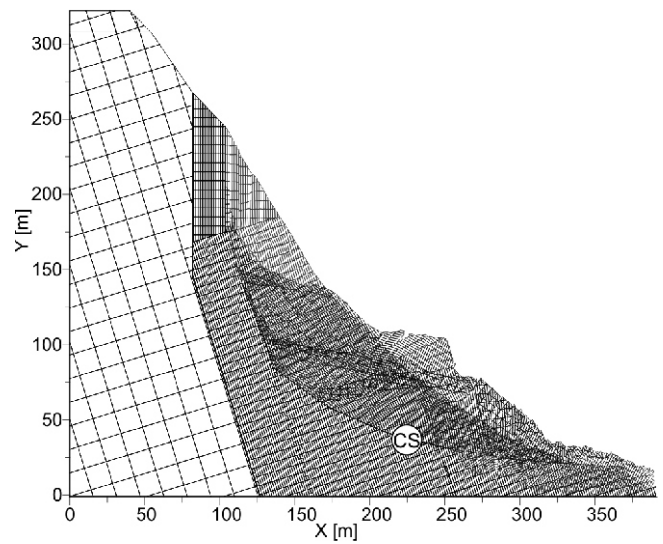


Fig. 12. Model III

Shape of the slope (dark grey) being the result of the numerical simulation over the original shape of the slope (light grey); explanations for Figures 10–13

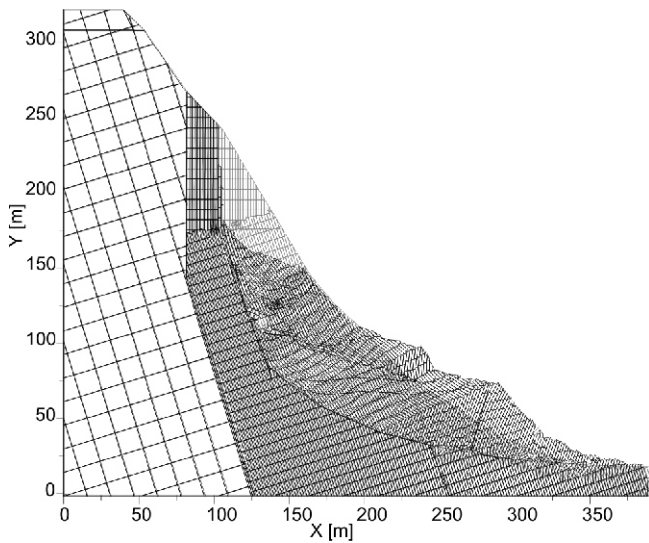


Fig. 11. Model II

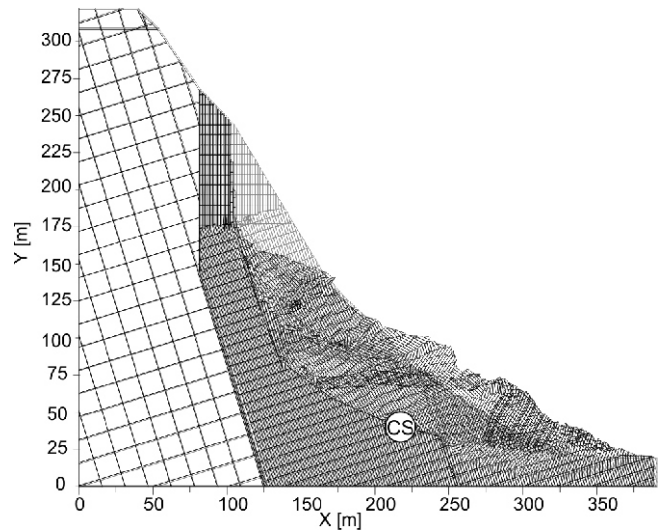


Fig. 13. Model IV

simulation was stopped. However, deformation processes were significantly advanced and only minimal residual deformation was still ongoing. Figures 10–13 show, for each model, the simulated landslide in dark grey overlying the original slope in light grey.

MODEL I

A slip surface develops in the lower part of the slope. Some new discontinuities appear as a consequence of slope displacements. Sliding of the blocks occurs along a surface which is in agreement with the structure of the rock mass. Numerous smaller block configurations are created, with distinctly differentiated inclinations of discontinuities. Discontinuous structures dominate and these significantly change the original shape of

the slope. The moving rock mass undergoes loosening and therefore the volume of the mass lying above the original slope is larger than the volume of the mass lying below it. The height of the zone elevated above the original terrain in the lowest part of the slope is ~40 m. The main scarp of the landslide is almost vertical, and the deposit in the lowest zone is relatively steep.

MODEL II

Numerous smaller structural features are developed in the central part of the slope (above the lowest continuous surface marked CS, shown in the figure). The orientations of the discontinuities have changed and are significantly different than the initial ones. The toe of the slope is less steep than in model I.

A few irregularities are visible on the slope surface, such as grooves, ridges and bulges. The rock mass in the deformed zones is highly loosened and therefore a large amount of material lies above the original slope shape.

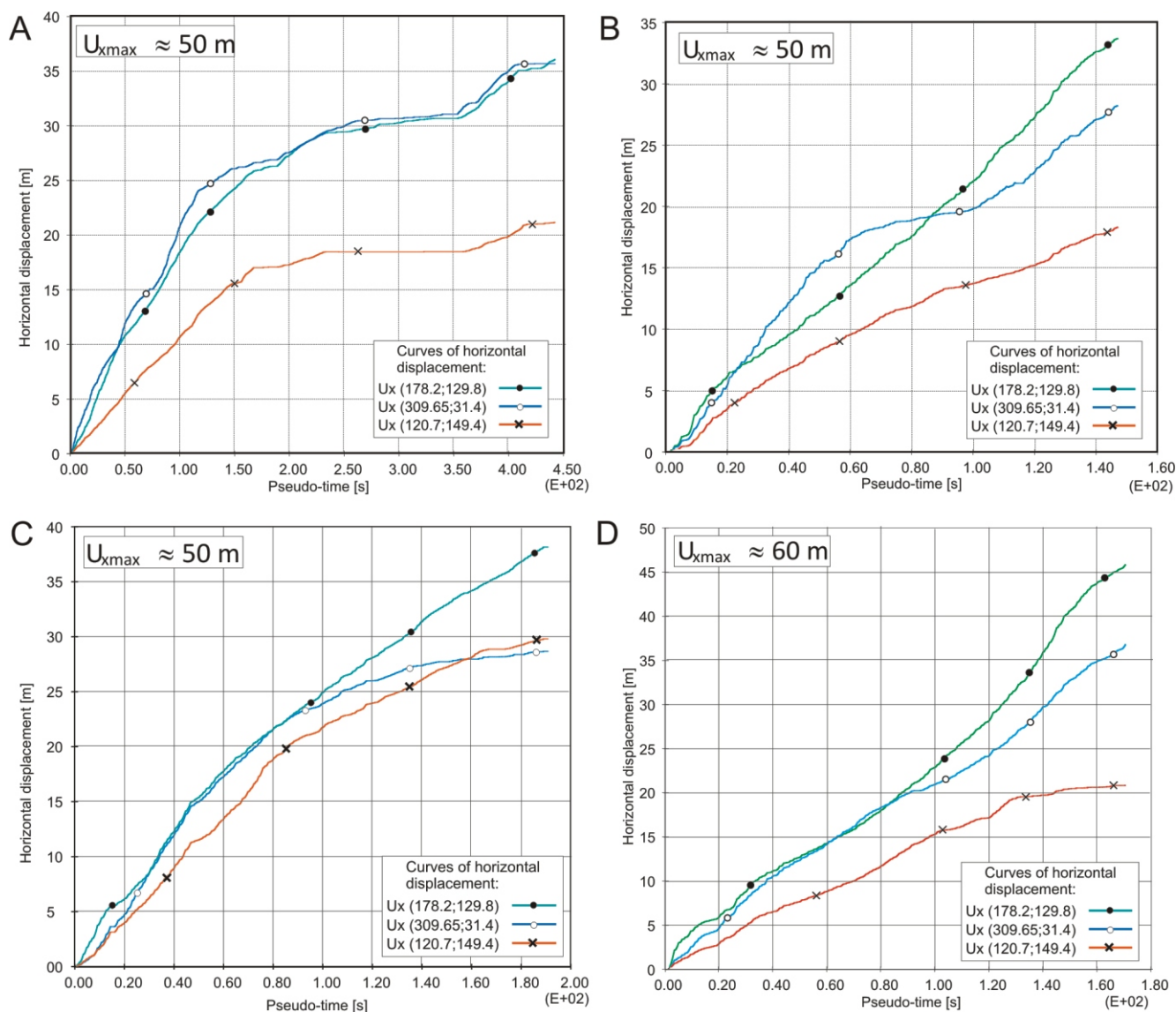


Fig. 14. Curves of horizontal displacement registered in selected points (see Fig. 9)

A – model I, B – model II, C – model III, D – model IV

#### MODEL III

The surface of the landslide deposit is more irregular than in the previous models. In the middle part of the deposit a large bulge formed and the limestone layers were buckled. The toe of the deposit is ~50 m long and relatively flat compared to those in the previous models. As can be seen, the zone below the large continuous slip surface (CS) at approximate coordinates  $X = 250\text{--}350$  m,  $Y = 0\text{--}25$  m is strongly disturbed, i.e. the block positions and inclinations of discontinuities are very irregular.

#### MODEL IV

Many smaller irregular landforms formed with different discontinuity inclinations. Blocks in the lowest part underwent distinct rotation. This is clearly visible in the lowest part of the slope, where the inclination angle of layers changed from the initial  $105$  to  $\sim 70^\circ$ .

The rock mass underwent more intensive loosening than in the case of square blocks and the volume of the mass above the original shape of the slope is significantly larger than the volume below it. The main scarp of the landslide is vertical and the

shape of its lower part is curvilinear. A slight inclination of the terrain in the central part of the slope is an effect of deformation occurring during the later stage of the process. The most significant loosening took place in the lower zone of the slope, where grooves, bulges and scarps formed at approximate coordinates  $X = 260$  m,  $Y = 100$  m and  $X = 175$  m,  $Y = 145$  m. Buckling of some layers is also clearly visible.

## DISCUSSION OF THE RESULTS

Four models were analysed, differing in rock block dimensions and in discontinuity parameters. Clearer and more detailed information concerning the deformation processes shown by the models can be achieved by analysis of the horizontal displacement curves. Displacement was registered in three reference points situated on the slope in the same position in all models (see Fig. 9):

**Model I.** The upper and middle part of the slope moved at similar rates, whereas the lower part underwent slow but significant stabilization, i.e. with displacement increments diminishing vs. time of the simulation (Fig. 14A);

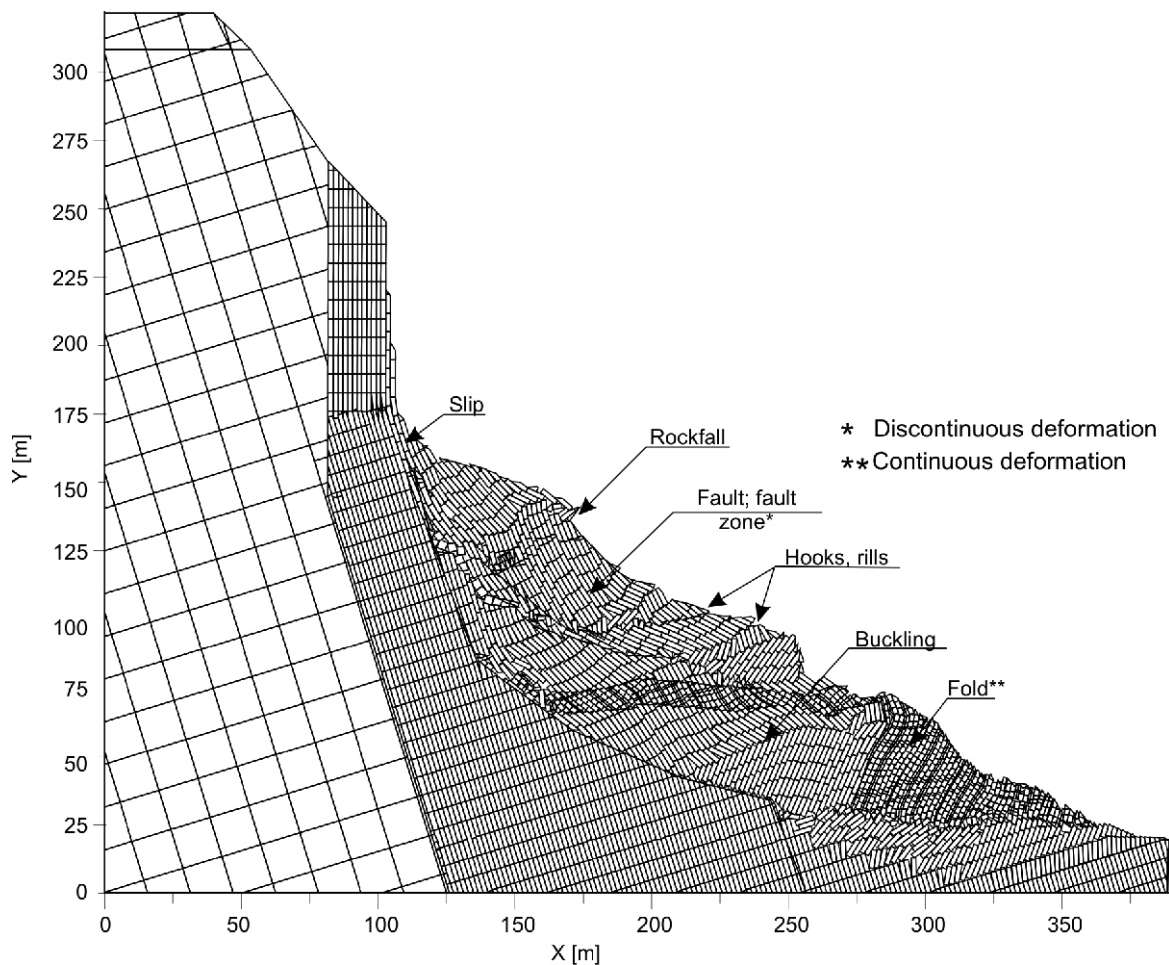


Fig. 15. Potential landslide resulting from the numerical simulation – model IV as an example

the simulation duration (~4500 seconds on the pseudo-time axis) was approximately three times longer than the durations of the other three models. This is due to higher parameters assigned to the discontinuities as well as to the shape and dimensions of the elementary blocks, indicating that the influence of interlocking of the blocks on the rate of mass failure is significant;

**Model II.** The lower part of the slope in the initial stage moves faster than the middle and upper parts, and its movement becomes slower in more advanced simulation stages. The movement of the middle zone in the later stages is most prominent (Fig. 14B). Lower geomechanical parameters of the discontinuities in the limestone and debris are the reason for the lack of stabilization signs in all parts of the slope;

**Model III.** Unlike in the above two cases, all parts of the slope in the initial stages move at approximately the same rate (Fig. 14C) and the lower part stabilizes slightly later; it seems that the reason lies in the rotation of the large packet of blocks in this part (see Fig. 12);

**Model IV.** The largest displacements occurring in the middle and lower parts (Fig. 14D) in comparison to those obtained in the other three models show that the rate of the landslide movement is highest in this model; the relative stabilization of the upper part results from the dominance of vertical displacements.

## CONCLUSIONS

In numerical analysis of a potential landslide involving jointed rock materials, four models of the slope selected were analysed using the Distinct Element Method. The models differ in the parameters assigned to the discontinuities and in the elementary block size and shape. The main conclusions drawn from this exercise are summarized below:

- The dominant movement observed is sliding along interbedding discontinuities.
- Nevertheless, different deformation and failure mechanisms can also take place within the deforming mass. These can be either discontinuous, such as buckling, fall, rotation of individual blocks, or continuous, such as plastic deformation.
- The shape of the blocks has an influence on the deformation mechanisms. Rectangular blocks result in a higher variability of landsliding processes than do square blocks. Smaller blocks, such as those in the debris accumulation at the base of the slope, are involved in continuous plastic deformation.
- The main landslide scarp has almost the same shape and similar dimensions in each model.
- A small decrease in the geomechanical parameters of the bedding discontinuities (see Tables 3 and 4) has a

significant influence on the simulation process and results. For instance, model I required a simulation duration almost three times longer (4500 s vs. 1700 s) than models II and IV, to obtain similar displacements. This result indicates the difficulty of evaluating further landslide deformation processes due to the sensitivity of the model to discontinuity parameters and elementary block shape and size.

- In all simulations, the rock mass undergoes a strong loosening in the deformed zones. This results from widening of the discontinuity apertures as the rock mass is collapsing and this is typical of rock masses composed of blocks of hard rock. Therefore, the volume of the landslide accumulation is larger than the original vol-

ume of the undisturbed rock mass before its deformation and displacement.

**Acknowledgements.** The publication is an product of multi-annual cooperation between the Research Institute for Geo-Hydrological Protection of the National Research Council in Italy and the Institute of Hydro-Engineering of the Polish Academy of Sciences. The authors thank the authorities of both institutes for financial and scientific support of their research. Moreover, the authors are grateful to all colleagues for valuable discussions and their fruitful comments and advice during preparation of this paper. Our deep appreciation is expressed to the reviewers, Prof. A. Wójcik from the Polish Geological Institute and an anonymous reviewer, who helped us to properly modify and to substantially improve the manuscript.

## REFERENCES

- Bieniawski, Z.T., 1984.** Rock Mechanics in Mining and Tunneling. A.A. Balkema, Rotterdam/Brookfield.
- Bossi, G., Zabuski, L., Pasuto, A., Marcato, G., 2016.** Capabilities of Continuous and Discontinuous Modelling of a Complex, Structurally Controlled Landslide. *Geotechnical and Geological Engineering*, <http://link.springer.com/article/10.1007/s10706-016-0057-z>
- Codeglia, D., 2013.** Analisi numerica tridimensionale tramite modello SPH della frana di Passo della Morte (UD) (in Italian). Unpublished M.Sc. thesis. University of Bologna, Italy.
- Codeglia, D., 2017.** Development of an Acoustic Emission Waveguide-based System for Monitoring of Rock Slope Deformation Mechanisms. Ph.D. thesis, Loughborough University.
- Codeglia, D., Dixon, N., Bossi, G., Marcato, G., 2017.** Alpine landslide risk scenario: run-out modelling using a 3D approach. *Rendiconti Online Società Geologica Italiana*, **42**: 14–17.
- Cundall, P.A., Hart, R.D., 2014.** Numerical modeling of discontinua. *Comprehensive Rock Engineering* **2**: 231–243.
- Giani, G.P., 1992.** Rock Slope Stability Analysis. A.A. Balkema, Rotterdam/ Brookfield.
- Hoek, E., Bray, J.D., 1981.** Rock Slope Engineering, 3rd edition. Taylor & Francis Group., London, New York.
- Itasca Consulting Group, Inc., 2004.** UDEC Manual. Itasca Consulting Group Inc.
- Marcato, G., Silvano, F., Zabuski, L., 2005.** Modellazione di ammassi rocciosi instabili con il metodo degli elementi distinti (in Italian). *Giornale di Geologia Applicata*, **2**: 87–92.
- Marcato, G., Zabuski, L., Silvano, S., 2007.** Capabilities of continuous and discontinuous modelling of the rock slopes – a landslide in the Carnian Alps (Italy) using as an example. *Geophysical Research Abstracts*, **9**: 02371. European Geosciences Union.
- Starfield, A.M., Cundall, P.A., 1988.** Towards a methodology for rock mechanics modelling. *International Journal of Rock Mechanics and Mining Sciences*, **25**: 99–106.
- Zabuski, L., Marcato, G., 2014.** Analysis of deformation processes of slopes with taking into account discontinuous character of the rock mass (in Polish with English summary). *Przegląd Geologiczny*, **62**: 308–316.